

Electronic Supplementary Information

A Polyoxometalate-Based Manganese Carboxylate Cluster

*Xikui Fang and Paul Kögerler**

Physical Measurements:

Infrared spectra (KBr pellets) were collected on a Bruker Tensor 27 instrument. Atmosphere compensation (CO₂ and H₂O) and baseline corrections (rubberband method) were carried out after spectrum collections. The ³¹P and ¹H NMR data were collected on a Varian VXR-400 MHz instrument. Typical sample concentrations were 0.2 – 0.5 mM. Elemental analysis results (ICP-OES) were obtained from Zentralabteilung für Chemische Analysen, Forschungszentrum Jülich GmbH, D-52425 Jülich, Germany.

Magnetic measurements and calculations:

A polycrystalline powder of **1** was used to measure the magnetic properties. The dc magnetic susceptibility of **1** was measured at 0.1 Tesla in the temperature range 2 – 290 K using a SQUID magnetometer (MPMS-5, Quantum Design) and corrected for diamagnetic contributions (estimated both from tabulated constants and measurements on diamagnetic polyoxotungstate precursors, $\chi_{\text{dia}}(\mathbf{1}) = -1.55 \times 10^{-3} \text{ emu mol}^{-1}$). Magnetization measurements at 2.0 K (0.1 – 5.0 Tesla) indicate the presence of 3.2 % of a mononuclear Mn⁴⁺ species per formula unit.

Best-fitting parameters ($J_1 - J_4$) were obtained using a modified version of the MAGPACK program package (J. J. Borrás-Almenar, J. M. Clemente-Juan, E. Coronado and B. S. Tsukerblat, *J. Comput. Chem.*, 2001, **22**, 985) that employs a Levenberg-Marquardt least-squares minimization mechanism for a predefined range of variables.

Control experiment using the $\{P_2W_{17}\}$ precursor:

Synthetic details: A sample of $[CeMn_6O_9(O_2CCH_3)_9(NO_3)(H_2O)_2]$ (**2**)¹ (0.20 g, 0.13 mmol) was dissolved in a mixture of 1:3 (v/v) CH_3COOH/H_2O (20 mL). With vigorous stirring, solid $K_{10}[\alpha_2-P_2W_{17}O_{61}]\cdot 20H_2O$ (0.64 g, 0.13 mmol) was then added to the above solution all at once. After stirring for 2 h at room temperature, dimethylamine hydrochloride (0.20 g) was added. The mixture was then heated in a 70 °C oil bath for another 15 min, filtered hot, and left to slowly evaporate at room temperature. After ca. 10 h, yellow plate crystals started to form and yielded 0.12 g product after two days. The yellow product was identified by single-crystal X-ray analysis as the 2:1 Weakley complex (shown below), $[\{\alpha_2-P_2W_{17}O_{61}\}_2Ce]^{16-}$. The cell parameters: triclinic *P*-1, $a = 26.486(3)$, $b = 26.518(3)$, $c = 26.560(3)$ Å, $\alpha = 81.832(2)$, $\beta = 76.957(2)$, $\gamma = 72.762(2)^\circ$, $V = 17\,299(3)$ Å³, $T = 173(2)$ K, $Z = 4$.

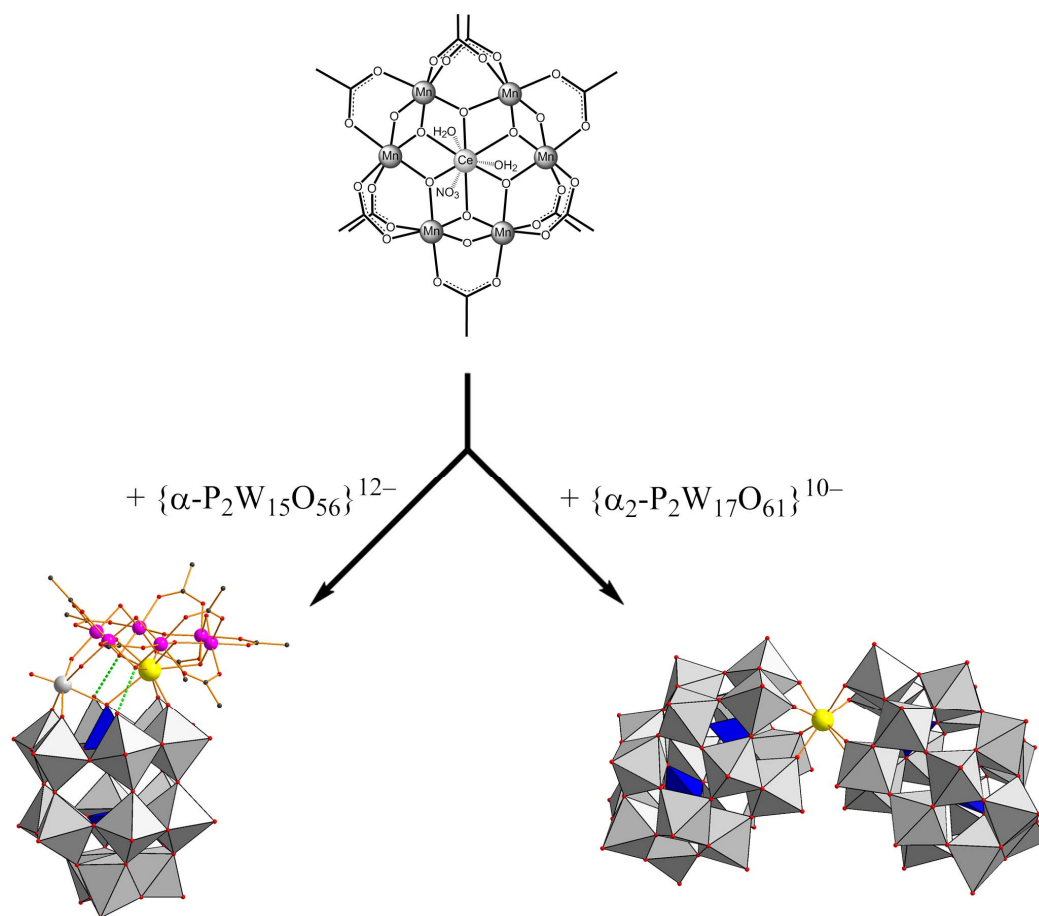


Figure S1. The reactions of the $\{CeMn_6\}$ cluster and two different Wells-Dawson polyoxoanion ligands: tri-vacant $[\alpha-P_2W_{15}O_{56}]^{12-}$ or mono-vacant $[\alpha_2-P_2W_{17}O_{61}]^{10-}$.

The mono-vacant $[\alpha_2\text{-P}_2\text{W}_{17}\text{O}_{61}]^{10-}$ anion generally accommodates a single metal ion in a tetradentate (for large lanthanide ions) or pentadentate fashion (for smaller transition metal ions). It is therefore expected that the coordination between $[\alpha_2\text{-P}_2\text{W}_{17}\text{O}_{61}]^{10-}$ and the $\{\text{CeMn}_6\}$ carboxylate cluster is initiated by binding to the Ce center since its terminal ligands (one nitrate and two aqua ligands) are weakly bound. On the other hand, the incorporation of a Mn ion is unlikely because it involves breaking multiple strong Mn–O bonds in order to free a single Mn(IV) ion. Once the Ce- $[\text{P}_2\text{W}_{17}]$ coordination is established, a concomitant weakening and subsequent breaking of the connection between Ce and the Mn_6 cluster unit occurs. This enables the coordination of a second $[\text{P}_2\text{W}_{17}]$ ligand to the Ce center and generates the 2:1 Weakley complex.

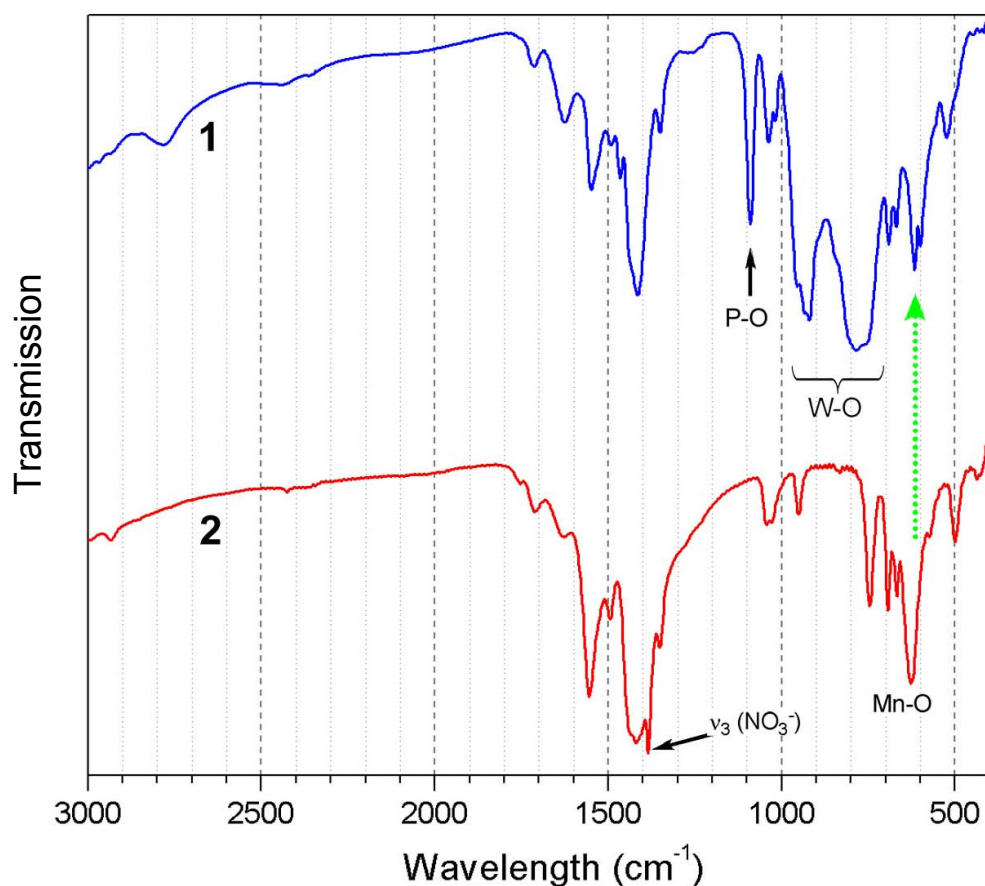


Figure S2. Comparison of the IR spectra of **1** and **2**. The overall structural effect of the described ligand exchange lowers the local symmetry of $\{\text{CeMn}_6\}$ core from approximately C_{3v} to C_s . This subtle structural change is reflected by the splitting of the Mn–O stretching band at 628 cm^{-1} into two peaks (green arrow, 617 cm^{-1} and 600 cm^{-1}). The NO_3^- ν_3 stretching frequency at 1385 cm^{-1} in **2**, characteristic of NO_3^- , is missing in **1**, confirming the absence of the nitrate group.

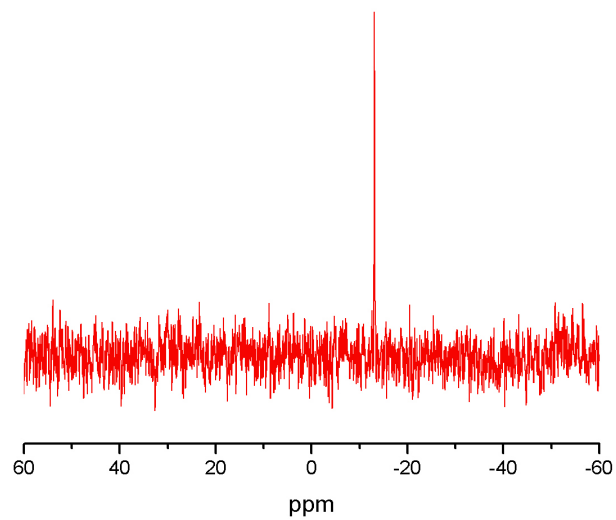


Figure S3. ^{31}P NMR spectrum of **1** in 1:3 $\text{CD}_3\text{COOD}/\text{D}_2\text{O}$ (0.5 mM).

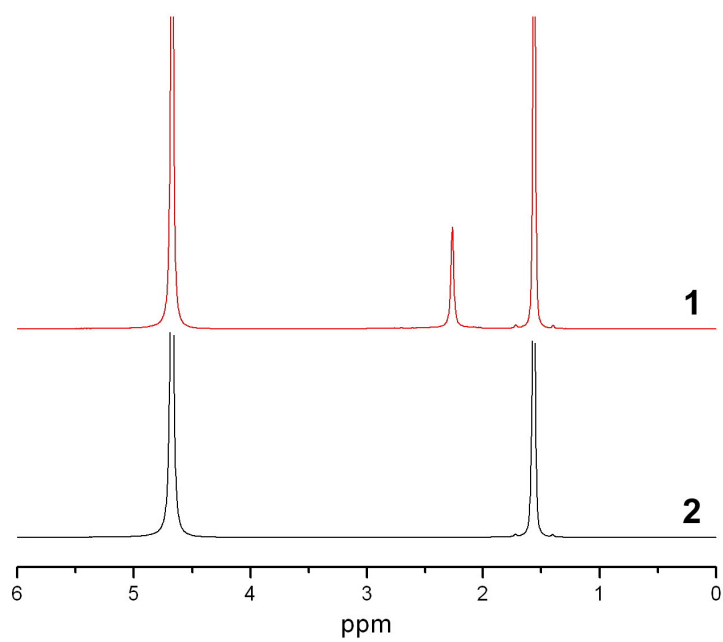


Figure S4. ^1H NMR spectra of **1** and **2** in 1:3 $\text{CD}_3\text{COOD}/\text{D}_2\text{O}$ (~0.2 mM).

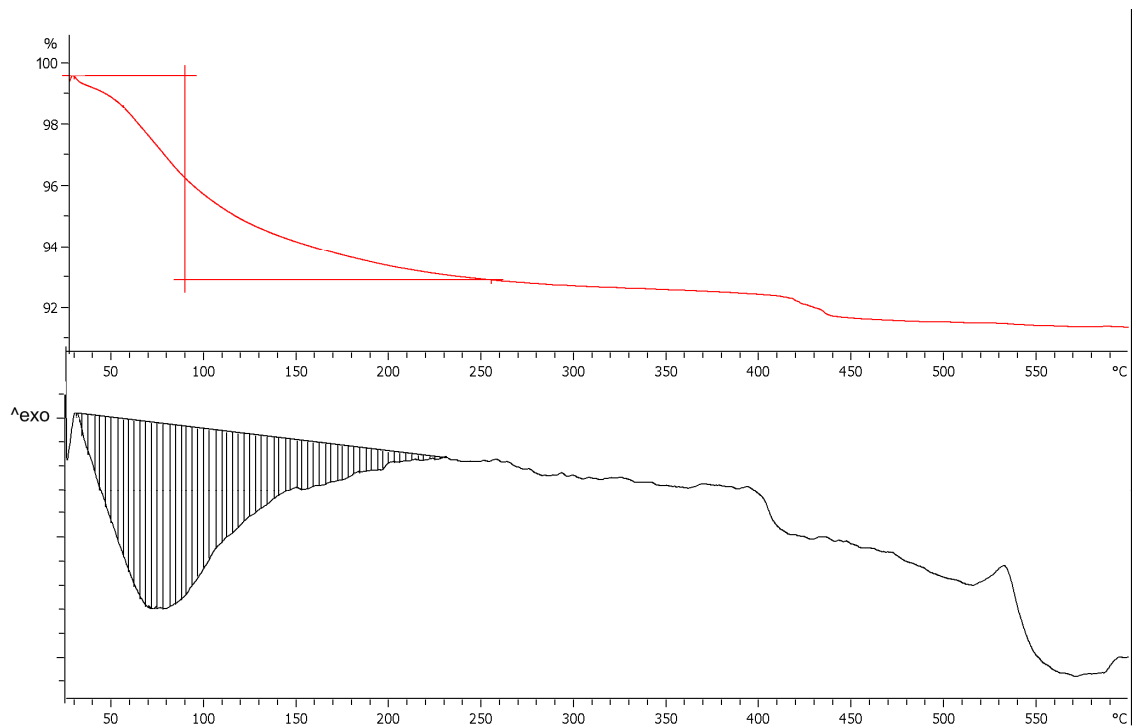


Figure S5. TGA and simultaneous DTA diagrams of **1** (10 K/min, 60 ml N₂/min). The highlighted first mass loss step is endothermic and corresponds to the loss of 20 molecules of crystal water per formula unit.

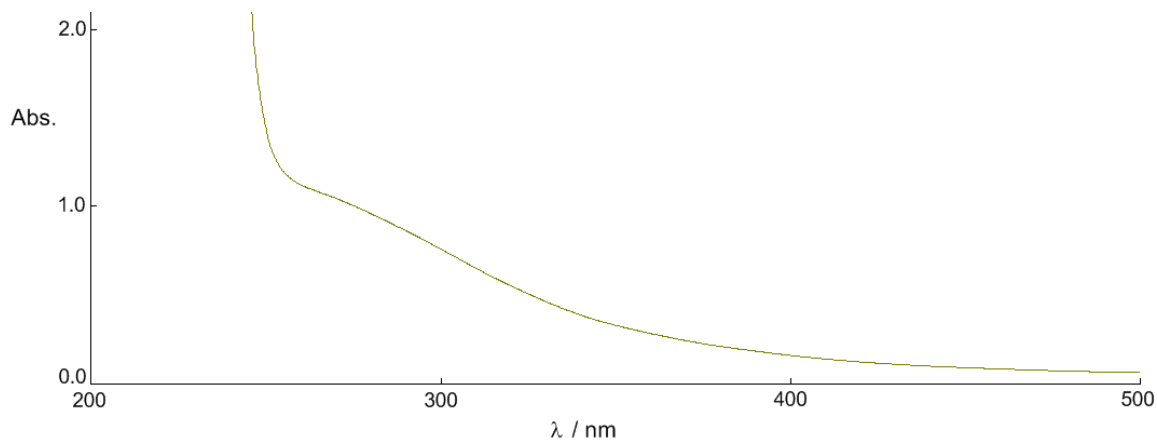


Figure S6. Electronic absorption spectrum of **1** (1:3 CH₃COOH/H₂O solution).

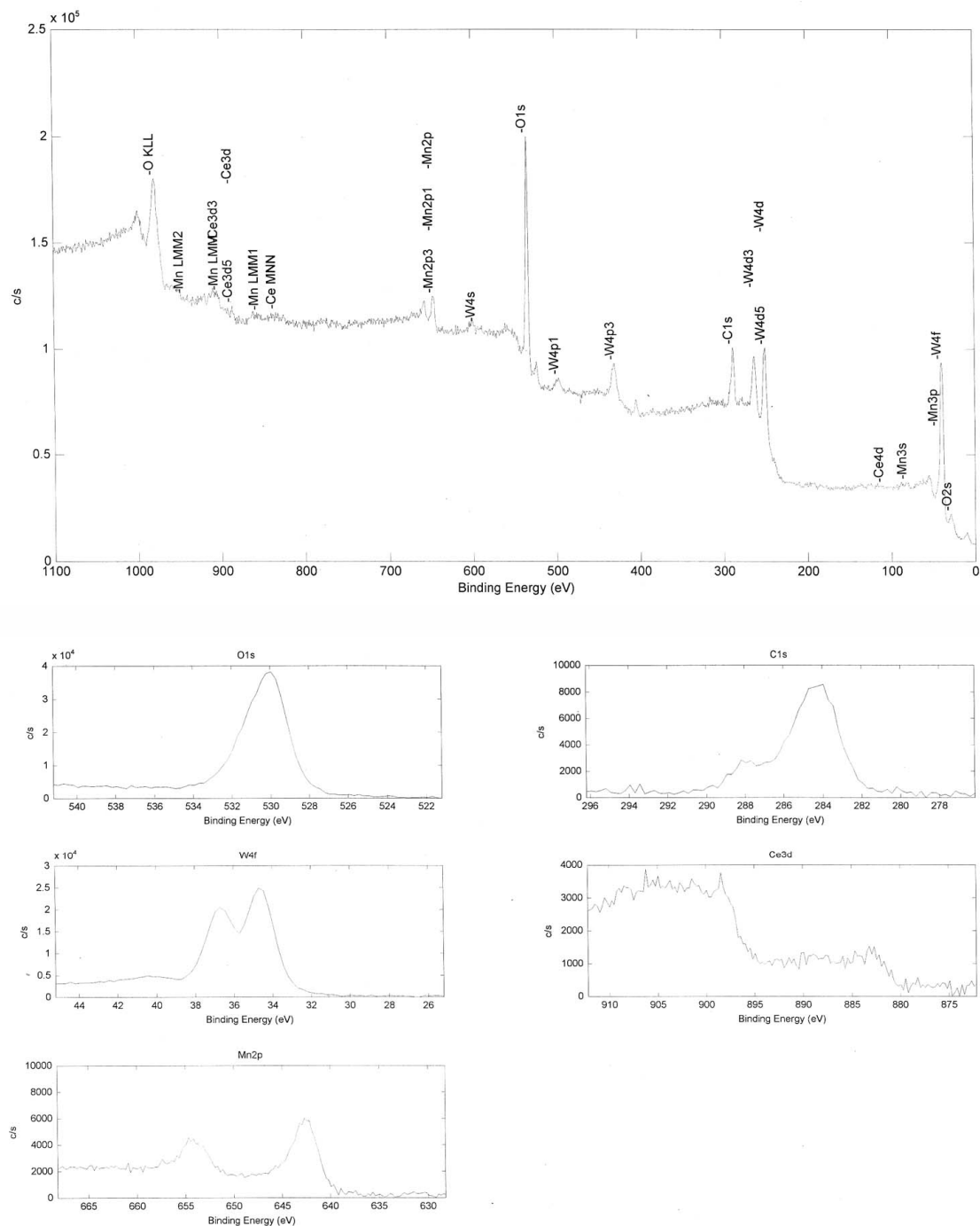


Figure S7. X-ray photoelectron spectrum of **1** (top) with the characteristic core level line of O, C, W, Ce and Mn shown individually (bottom); O 1s (at 530.0 eV) line is used as internal reference.

The Mn 2p spectrum includes a doublet with a spin-spin splitting of ~13 eV (654.8 eV, 2p_{1/2}; 642.7 eV, 2p_{3/2}). This is suggestive of a species with uniform Mn sites and consistent with the assignment that all 6 Mn sites are Mn(IV). However, it should be noted that the determination of the oxidation state as Mn(IV) solely based on the binding energy is subject to two limitations. First, the binding energy is known to be

dependent on the chemical environment. Second, the lack of the appropriate internal Mn reference peaks (i.e. a standard) complicates the precise determination of the chemical shift. Although we have used the O1s line (530.0 eV) as the internal reference in this current case, the oxygen 1s signal itself varies with the nature of the compound for the same reason mentioned above. On the other hand, due to the low concentration of Ce in the sample the Ce signals are too weak to yield significant information.

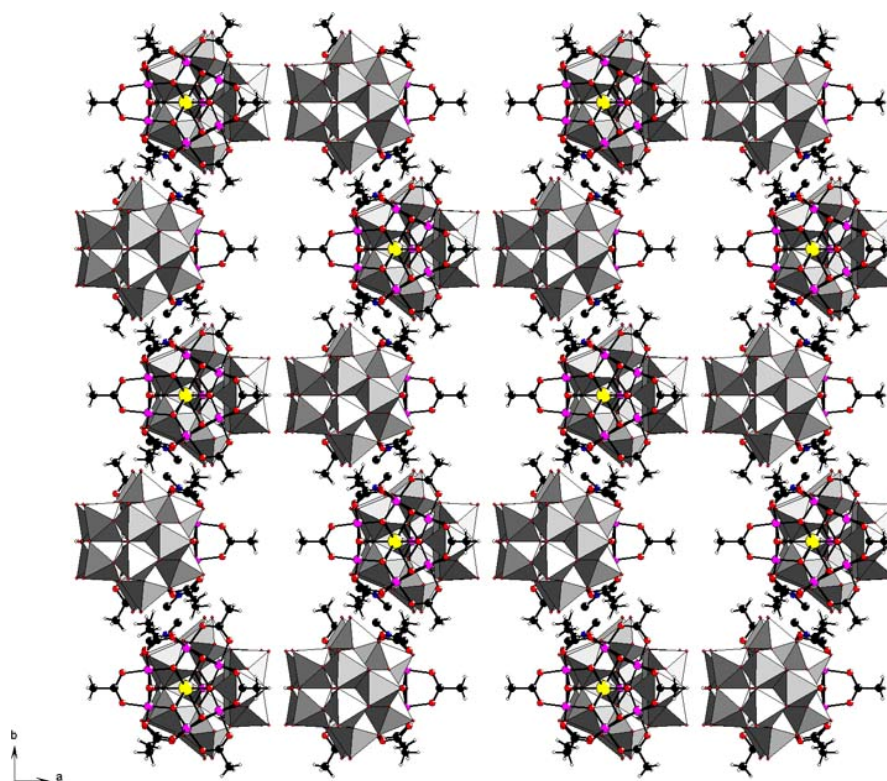


Figure S8. Packing diagram of **1** visualized along the crystallographic *c*-axis. The counteranions and crystal solvent water molecules have been omitted for clarity.